Photochemical *trans–cis* isomerisation of donor/acceptor-substituted (*E*)-hex-3-ene-1,5-diynes (1,2-diethynylethenes, DEEs) and 3,4-diethynylhex-3-ene-1,5-diynes (tetraethynylethenes, TEEs)

Rainer E. Martin,[a] Johannes Bartek,[a] François Diederich,*[,a] Rik R. Tykwinski,†[,a] Erich C. Meister,[b] Anouk Hilger[c] and Hans Peter Lüthi[c]

[a] *Laboratorium für Organische Chemie, ETH-Zentrum, Universitätstrasse 16, CH-8092 Zürich, Switzerland*
[b] *Laboratorium für Physikalische Chemie, ETH-Zentrum, Universitätstrasse 22, CH-8092 Zürich, Switzerland*
[c] *Swiss Center for Scientific Computing, ETH-Zentrum, Clausiusstrasse 59, CH-8092 Zürich, Switzerland*

The photochemically reversible *trans–cis* isomerisation of (*E*)-hex-3-ene-1,5-diynes (1,2-diethynylethenes, DEEs) and 3,4-diethynylhex-3-ene-1,5-diynes (tetraethynylethenes, TEEs) substituted with electron-donating (*p*-dialkylaminophenyl) and/or electron-accepting (*p*-nitrophenyl) groups has been examined. The type and degree of donor/acceptor (D/A) functionalisation has been found to drastically affect the partial quantum yields of isomerisation $\Phi_{t\rightarrow c}$ and $\Phi_{c\rightarrow t}$. Total quantum yields in *n*-hexane vary from $\Phi_{total} = 0.72$ for a bis-acceptor substituted TEE to $\Phi_{total} = 0.015$ for a four-fold, bis-donor, bis-acceptor substituted TEE derivative. A strong relationship between Φ_{total} and solvent polarity as well as a strong dependence of $\Phi_{t\rightarrow c}$ and $\Phi_{c\rightarrow t}$ on the wavelength of excitation λ_{exc} has been observed. The temperature dependence of the photoisomerisation has been investigated for a bis-acceptor-substituted DEE and shows no changes in Φ_{total} over the temperature range 6.5–65 °C. None of the compounds studied undergoes thermal isomerisation at 27 °C in *n*-hexane. Further analysis of these compounds by theoretical investigations at the semiempirical level of theory reveals a significant reduction of the bond order of the central olefinic double bond in the D–D, D–A and A–A TEEs upon electronic excitation, thus ultimately facilitating photoisomerisation.

The ability to control and dictate and photochemical *trans–cis* isomerisation about an olefinic double bond is appealing for the creation of dynamic systems for use as energy storage networks or as molecular switches, hinges and probes.[1–4] Furthermore, it has been suggested that photoreversible *trans–cis* interconversion about double bonds in certain tetrapyrroles also plays an essential role in manifold processes involved in the growth of plants.[5] More recently, practical applications of functional, bistable olefins have been found in systems such as the chir-optical switches introduced by Feringa and co-workers.[1,6] The principles of olefin isomerisation have been extensively explored, in particular for stilbene[7,8] and azobenzene[9] derivatives.

To a first approximation, the photochemical *trans–cis* interconversion between two geometric isomers appears to be a straightforward process. This is seldom the case, however, since variables such as solvent, steric factors, stability, functionality and temperature all play crucial roles. Furthermore, mechanistic considerations for olefinic isomerisations are complicated by competing processes such as fluorescence, intersystem singlet–triplet crossing, and the potential participation of intermediate phantom or twisted intramolecular charge transfer (TICT) states.[10] Thus, the study of *trans–cis* isomerisation continues to attract attention as a seemingly simple, yet challenging and rewarding field of research.[11]

As mentioned, the photochemical behaviour of stilbenes as it relates to *trans–cis* isomerisation processes has been widely studied from both theoretical and experimental viewpoints.[8] These molecules are a practical choice for such studies due to facile synthetic routes, stability and varied electron donating and/or accepting functionalities.[12] In the case of (*Z*)-stilbene or tetraphenylethene derivatives, the close proximity of aryl moieties results in steric interactions which undoubtedly influence the electronic and photonic characteristics of these molecules. 1,2-Diethynylethenes [DEEs, (*E*)-hex-3-ene-1,5-diynes] and tetraethynylethenes (TEEs, 3,4-diethynylhex-3-ene-1,5-diynes) with electron donating (*p*-dialkylaminophenyl) or electron accepting (*p*-nitrophenyl) substituents [(*E*)-**1** and (*Z*)-**1**, Scheme 1] are two classes of highly stable molecules that are available from straightforward and high yielding synthetic protocols and are amenable to versatile and diverse functionalisation.[13,14] The expanded, conjugated enyne framework of DEEs and TEEs sets these compounds apart from the corresponding stilbenoid chromophores. The aryl rings with the pendant donor and/or acceptor (D/A) functionalities are sufficiently remote from each other to preclude unfavourable steric interactions during the course of *trans–cis* isomerisations, and thus electronic effects can be isolated from steric effects. Indeed, X-ray structural analysis of a *cis*-bis-arylated D–A TEE showed that planarity is maintained across the entire conjugated chromophore including the aryl rings.[14b] The advantages of these unique compounds have been documented through investigations of their thermal stability,[14] electrochemical behaviour[15] and non-linear optical responses.[16,17] These studies revealed that the physical characteristics of DEEs and TEEs can be significantly manipulated by the appropriate choice of donor and/or acceptor substituents.

The behaviour of functionalised DEEs and TEEs under photochemical irradiation is of critical importance for the use of these molecules in device construction and other practical applications. With this in mind, we have investigated the photoisomerisation characteristics for two series of donor–donor (D–D), acceptor–acceptor (A–A) and donor–acceptor (D–A)

† Current address: Department of Chemistry, University of Alberta, Edmonton, Alberta T6G 2G2, Canada.

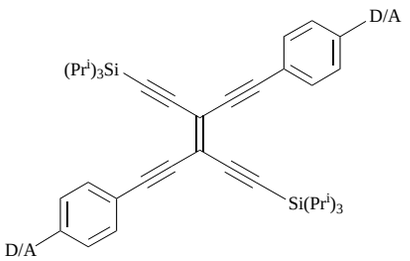

(*E*)-**1**

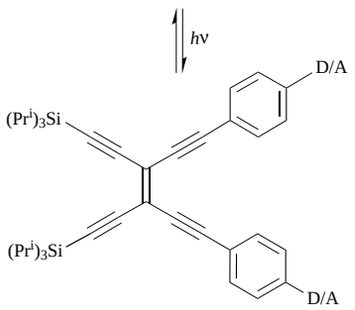

(*Z*)-**1**

D = donor, A = acceptor

Scheme 1 Photochemical *trans–cis* isomerisation in donor/acceptor substituted tetraethynylethenes (TEEs)

substituted DEEs [(*E*)-**2**–(*E*)-**4**] and TEEs [(*E*)-**5**–(*E*)-**8**] with respect to structure, solvent and temperature. In some ways these compounds display a behaviour similar to that of analogously substituted stilbenes; thus D–A substituted DEEs and TEEs, in analogy with stilbenes such as (*E*)-**9**, prefer the *cis*-configuration upon irradiation in apolar solvents. In other ways, however, our results clearly show that the unencumbered framework of DEEs and TEEs imparts unique characteristics to these chromophores, despite their structural similarity to stilbene analogs. The expanded chromophores do not undergo thermally induced isomerisation, and the solvent and excitation wavelength dependence of their photoinduced *trans–cis* isomerisation differs strongly from that reported for stilbenes.

Results and discussion

Structure dependence

The photochemical *trans–cis* isomerisation of the donor and/or acceptor substituted DEEs and TEEs (*E*)-**2**–(*E*)-**8** was probed *via* monochromatic irradiation of dilute *n*-hexane solutions (*ca.* 2–4 × 10^{-5} M) at 27 °C (Table 1). The excitation wavelength (λ_{exc}) normally corresponded to the lowest energy absorption maximum (λ_{max}) in the UV–VIS spectrum of each molecule.[14a,b] In the case of tetrakis-arylated TEE (*E*)-**8**, however, higher energy excitation (λ_{exc} = 390 nm) was required since irradiation at λ_{max} (528 nm) over a period of 18 min at maximum light intensity[18] resulted in negligible isomerisation to (*Z*)-**8**. The evaluation of quantum yields from experimental data for (*E*)-**3**–

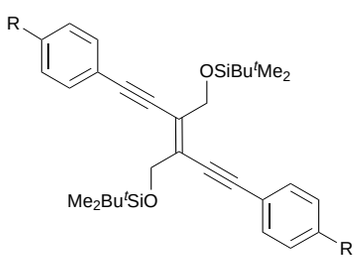

(*E*)-**2**, R = NMe$_2$
(*E*)-**3**, R = NO$_2$

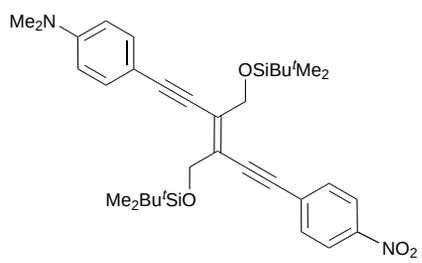

(*E*)-**4**

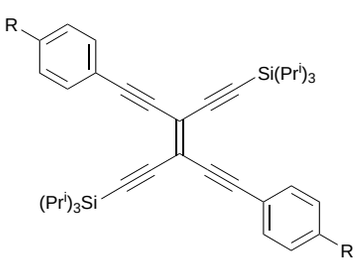

(*E*)-**5**, R = NMe$_2$
(*E*)-**6**, R = NO$_2$

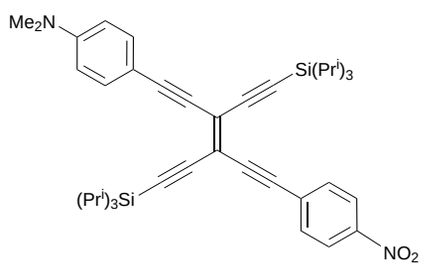

(*E*)-**7**

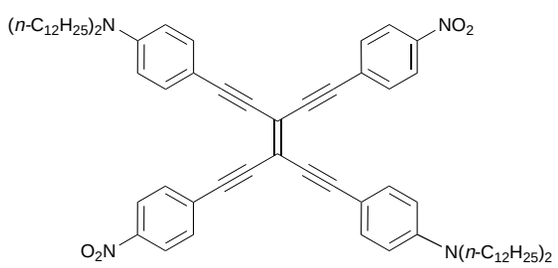

(*E*)-**8**

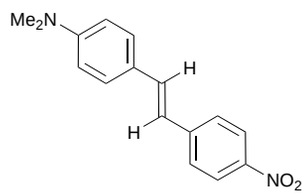

(*E*)-**9**, DANS

Table 1 Results of the photochemical *trans–cis* isomerisation of functionalised DEEs [(*E*)-**3**, (*E*)-**4**] and TEEs [(*E*)-**5**–(*E*)-**8**] in *n*-hexane at 27 °C

Compound	λ_{exc}/nm	% *trans*[a]	% *cis*[a]	K_{photo}^{eq}[b]	$\Phi_{t\rightarrow c}$	$\Phi_{c\rightarrow t}$	Φ_{total}	$\Phi_{t\rightarrow c}/\Phi_{c\rightarrow t}$	$t_{\frac{1}{2}}$/min[c]
(*E*)-**3**	360	45.5	54.5	1.2	0.14	0.27	0.41	0.5	9
(*E*)-**4**	405	2.9	97.1	33.5	0.080	0.0080	0.088	10.0	27
(*E*)-**5**	450	59.7	40.3	0.7	0.072	0.18	0.25	0.4	29
(*E*)-**6**	416	57.5	42.5	0.7	0.29	0.43	0.72	0.7	6
(*E*)-**7**	451	10.8	89.2	8.3	0.025	0.0052	0.030	4.8	101
(*E*)-**8**	390	68.3	31.7	0.5	0.0027	0.012	0.015	0.2	276

[a] At photostationary state. [b] Photoequilibrium constant.[19] [c] Calculated for $I_0 = 1.0 \times 10^{-10}$ E s^{-1} cm^{-2}.

(*E*)-**8** is described in detail in the Experimental section. For the isomerisation of compounds (*E*)-**3**–(*E*)-**8**, well defined isosbestic points were obtained and no decomposition products were detected by UV–VIS spectroscopy or HPLC analysis. Only the D–D substituted DEE (*E*)-**2** entered into a secondary, undefined reaction pathway upon irradiation. Furthermore, this degradation was observed regardless of working with air-saturated or degassed solutions; therefore its photoisomerisation could not be studied quantitatively. Analysis of the isomeric ratio at the photostationary state by HPLC afforded the final *trans*- and *cis*-concentrations C_t^{eq} and C_c^{eq}, respectively, which were then used for the calculation of the partial rate constants $k_{t\rightarrow c}$ and $k_{c\rightarrow t}$, as well as the photoequilibrium constants K_{photo}^{eq}.[19] The partial rate constants, in combination with the irradiation light intensity I_0, the molar absorptivity $A_{\lambda_{exc}}^{eq}$ of the irradiated solution at the photostationary state and the molar decadic extinction coefficients of the pure isomers ε_t and ε_c at the wavelength of excitation ultimately afforded the partial quantum yields $\Phi_{t\rightarrow c}$ and $\Phi_{c\rightarrow t}$, respectively.

The electronic structure of the arylated DEEs and TEEs has a substantial impact on the ratio of *trans*- and *cis*-isomers at the photostationary state and on the partial quantum yields $\Phi_{t\rightarrow c}$ and $\Phi_{c\rightarrow t}$, for which changes of about two orders of magnitude were observed. The A–A substituted **3** and **6** showed by far the highest total quantum yields Φ_{total} of 0.41 and 0.72, respectively. Unfortunately, the decomposition of D–D substituted DEE (*E*)-**2** prevented direct comparison with its TEE counterpart (*E*)-**5**. By analogy with the bis-acceptor derivatives **3** and **6**, D–D substituted **5** displayed little preference for formation of the *trans*- or *cis*-isomer in the equilibrium product distribution, although the partial quantum yield $\Phi_{c\rightarrow t}$ was consistently higher than $\Phi_{t\rightarrow c}$ in all three cases.

The D–A functionalised molecules **4**, **7** and **8** showed the lowest total quantum yields with $\Phi_{total} = 0.088$, 0.030 and 0.015, respectively. In contrast to all other compounds, for which $\Phi_{c\rightarrow t}$ was about 2–5 times larger than $\Phi_{t\rightarrow c}$, a reversed trend was observed for D–A systems **4** and **7**, with $\Phi_{t\rightarrow c}$ being 10 and 5 times larger than $\Phi_{c\rightarrow t}$, respectively. As a consequence, compounds (*E*)-**4** and (*E*)-**7** were transformed almost completely into the *cis*-isomers. This results from the inability of the non-polar solvent *n*-hexane to stabilise the higher dipole of the *trans*-isomers in the excited state (*vide infra*). The tetrakis-arylated TEE **8** showed a 2:1 *trans*:*cis* ratio at the photoequilibrium state with $\Phi_{c\rightarrow t}$ being nearly five times that of $\Phi_{t\rightarrow c}$. In many aspects, the photochemical properties of chromophore **8**, despite its *cis*- and *gem*-D–A conjugation pathways, indeed resemble more closely those of *trans*-D–D (**5**) or *trans*-A–A TEE (**6**) than those of a *cis*-D–A TEE (**7**).

The rate at which the arylated DEEs and TEEs undergo isomerisation is of practical importance, since application of functional materials requires both structural homogeneity and stability. Under the assumption that the partial quantum yields $\Phi_{t\rightarrow c}$ and $\Phi_{c\rightarrow t}$ are independent of irradiation light intensity and chromophore concentration, half-life times $t_{\frac{1}{2}}$ for uniform irradiation intensity were calculated. These $t_{\frac{1}{2}}$ values for compounds (*E*)-**3**–(*E*)-**8** (Table 1) clearly highlight the influence of substitution on the rate of isomerisation; alternatively, $t_{\frac{1}{2}}$ can also be viewed as an indicator of relative 'photostability'. The A–A substituted (*E*)-**3** and (*E*)-**6** rapidly undergo isomerisation, displaying half-life times of mere minutes, whereas the D–D-TEE (*E*)-**5** and the D–A substituted (*E*)-**4** and (*E*)-**7** are consistently more resistant to isomerisation in *n*-hexane. The most retarded rate, with a $t_{\frac{1}{2}}$ of almost 5 h, was obtained for the tetrakis-arylated (*E*)-**8**.

The excitation wavelength λ_{exc} at which a molecule must be irradiated to undergo complete conversion from the *trans*-isomer to its *cis*-form is of great interest not only from a synthetic point of view but also for device construction.[7] The *trans*- and *cis*-isomers of compounds **3**–**8** have very similar absorption bands in their UV–VIS spectra, and thus even by using different excitation wavelengths λ_{exc}, a complete conversion from one isomeric form to the other can seldom be achieved. Besides the positions of the absorption bands, the partial quantum yields are also important since they dictate whether or not complete conversion can be expected. The D–A compounds **4** and **7** show the greatest disparity, with $\Phi_{c\rightarrow t} \ll \Phi_{t\rightarrow c}$. Indeed, irradiation at the longest wavelength absorption maximum λ_{max} of (*E*)-**4** and (*E*)-**7** caused nearly complete conversion to the *cis*-isomer.

The fact that Φ_{total} is significantly smaller than unity, especially for the D–A functionalised systems **4**, **7** and **8**, shows that major relaxation channels exist for the excited states that do not result in direct isomerisation. Fluorescence, among others, is one such well known competing pathway.[7,8b] The D–D and D–A molecules (*E*)-**2**, (*E*)-**4**, (*E*)-**5**, (*E*)-**7** and (*E*)-**8** displayed varying degrees of fluorescence in *n*-hexane,[14a] whereas for both A–A compounds (*E*)-**3** and (*E*)-**6**, no fluorescence was observed in this solvent. In fact, the isomerisation processes of **3** and **6** are by far the most efficient ($\Phi_{total} = 0.41$ and 0.72). The fluorescence processes of (*E*)-**4** ($\Phi_F = 0.13$) and (*E*)-**7** ($\Phi_F = 0.42$) are quite efficient,[14a] and accordingly, their isomerisation tendency is significantly reduced (**4**: $\Phi_{total} = 0.088$; **7**: $\Phi_{total} = 0.030$). Remarkably, although the fluorescence quantum yield Φ_F for the D–D derivative (*E*)-**5** is high ($\Phi_F = 0.53$),[14a] the second highest isomerisation rate within the TEE series is observed for this chromophore ($\Phi_{total} = 0.25$). The D–A substituted TEE (*Z*)-**7** also displayed a bright fluorescence in *n*-hexane ($\Phi_F = 0.12$). This contrasts the absence of fluorescence at ambient temperatures displayed by (*Z*)-stilbene derivatives, which has usually been explained by very short-lived first excited states.[8a,20] The rapid isomerisation of (*Z*)-stilbenes has been attributed to steric strain which is absent in the (*Z*)-DEE and (*Z*)-TEE derivatives. This structural difference could determine differences in excited state lifetimes and fluorescence quantum yields between the two classes of compounds.

The D/A-functionalised DEEs and TEEs exhibit a remarkably different photochemical behaviour as compared to corresponding stilbene molecules. A large variation of both partial quantum yields $\Phi_{t\rightarrow c}$ and $\Phi_{c\rightarrow t}$ as a function of substitution of the central core with donor and/or acceptor groups is observed. In contrast, to a first approximation, $\Phi_{c\rightarrow t}$ is independent of substitution about the stilbene framework, whereas $\Phi_{t\rightarrow c}$ shows considerable dependence upon changes in functionality. For example, in the non-polar solvent mixture methylcyclohexane–isopentane (2:1 v/v) the donor substituted (*E*)-4-dimethylaminostilbene exhibits a partial quantum yield for the isomerisation to the (*Z*)-derivative of $\Phi_{t\rightarrow c} = 0.52$.[21] In benzene for (*E*)-configured 4-(*N*,*N*-dimethylamino)-4-nitrostilbene (DANS) (**9**), 4,4′-dinitro-, 4-nitro-4′-methoxy-, and 4-nitro-4′-

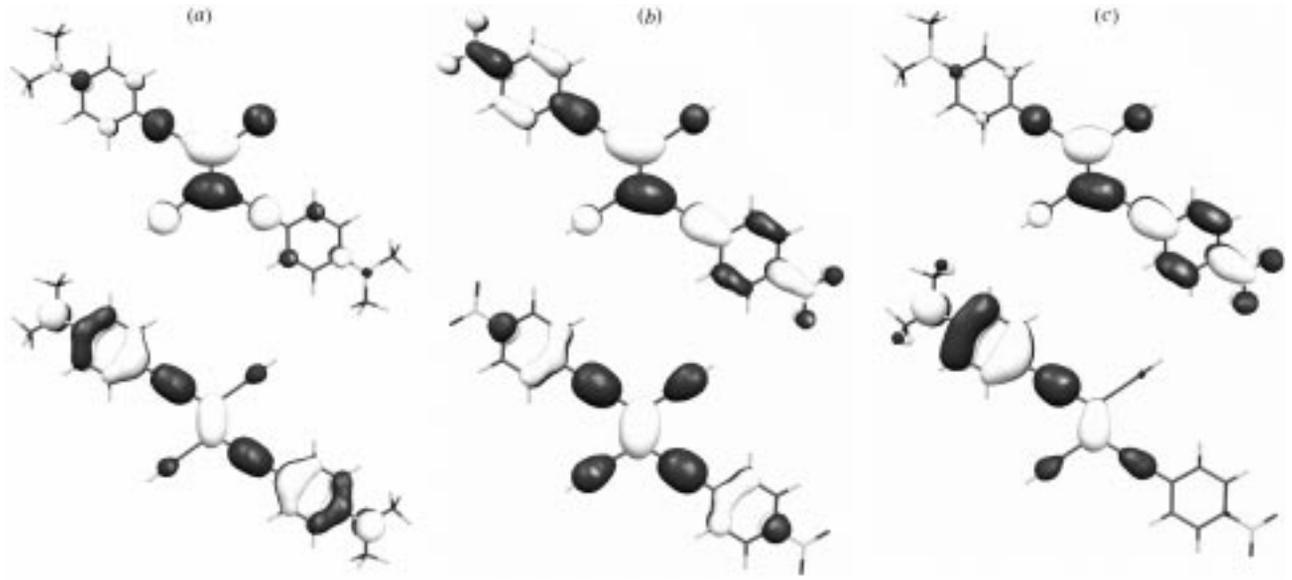

Fig. 1 Highest occupied molecular orbitals (HOMOs; bottom) and lowest unoccupied molecular orbitals (LUMOs; top) of (*a*) D–D substituted (*E*)-**5**, (*b*) A–A substituted (*E*)-**6** and (*c*) D–A substituted (*E*)-**7**. In the structures computed on the AM1-CI level of theory, the $Si(Pr^i)_3$ groups of (*E*)-**5**–(*E*)-**7** were replaced by H-atoms.

Table 2 Solvent dependence of the photochemical *trans–cis* isomerisation of D–A substituted TEE **7** at 27 °C

Compound	Solvent	λ_{exc}/nm	% *trans*[a]	% *cis*[a]	$K^{eq.}_{photo}$[b]	$\Phi_{t\rightarrow c} \times 100$	$\Phi_{c\rightarrow t} \times 100$	$\Phi_{total} \times 100$	$\Phi_{t\rightarrow c}/\Phi_{c\rightarrow t}$	Dipole moment[c]/C m
(*E*)-**7**	*n*-hexane	451	10.8	89.2	8.3	2.5	0.52	3.0	4.8	0
(*E*)-**7**	CCl_4	451	16.1	83.9	5.2	0.54	0.17	0.71	3.2	0
(*E*)-**7**	THF	451	29.3	70.7	2.4	0.14	0.092	0.23	1.5	5.7
(*E*)-**7**	EtOH	451	27.4	72.6	2.6	0.054	0.033	0.087	1.6	5.7
(*E*)-**7**	$CHCl_3$	451	30.2	69.8	2.3	0.038	0.023	0.061	1.7	3.7
(*E*)-**7**	CH_3CN	451[d]	100	0	—	0	—	—	—	11.7
(*Z*)-**7**	CH_3CN	473[d]	0	100	—	—	0	—	—	11.7
(*Z*)-**7**	CH_3CN	451[d]	0	100	—	—	0	—	—	11.7
(*E*)-**7**	CH_3CN	291	40.8	59.2	1.5	2.2	1.9	4.1	1.2	11.7
(*E*)-**7**	DMF	451[d]	100	0	—	0	—	—	—	*ca.* 12.7
(*Z*)-**7**	DMF	451[d]	0	100	—	—	0	—	—	*ca.* 12.7

[a] At photostationary state. [b] Photoequilibrium constant.[19] [c] From ref. 25. [d] Changes in absorption were too insignificant for evaluation of quantum yields.

aminostilbene, $\Phi_{t\rightarrow c} = 0.016$, 0.27, 0.40 and 0.10, respectively.[22] In contrast, for all mentioned stilbene derivatives $\Phi_{c\rightarrow t}$ varies in a much smaller range, as is illustrated by $\Phi_{c\rightarrow t} = 0.22$,[21] 0.40, 0.34, 0.43 and 0.44,[22] respectively.

Computational studies

As observed for most conjugated π-systems, there is a strong coupling between changes in electronic structure and changes in geometry. Therefore, consideration of the changes in electron density on the π-bonds gives a good indication of the geometric modifications occurring upon excitation.[23] Inspection of the wavefunction showed that the first excited state in the D–D, A–A and D–A substituted TEEs [(*E*)-**5**–(*E*)-**7**] originates mainly from an electron transition between the highest occupied molecular orbital (HOMO) and the lowest unoccupied molecular orbital (LUMO). For the analysis of the effects of substitution on the electronic structure for the series of D–D, A–A and D–A TEEs (*E*)-**5**–(*E*)-**7**, we thus focused on the consideration of the corresponding HOMOs and LUMOs.

The calculations for the ground state were performed at the semiempirical AM1 (Austin Model 1) level as implemented in AMPAC.[24] In the calculated structures, the $Si(Pr^i)_3$ groups of (*E*)-**5**–(*E*)-**7** were replaced by H-atoms.

In the D–D substituted (*E*)-**5**, strong delocalisation of the HOMO throughout the whole π-system is observed [Fig. 1(*a*)]. The LUMO, on the other hand, mainly shows localisation on the central olefinic bond, *i.e.* strong π*-antibonding character, and only weak delocalisation into the phenyl rings. The HOMO of the A–A substituted (*E*)-**6** reveals strong π-bonding character which is concentrated about the central TEE core [Fig. 1(*b*)]. The LUMO displays strong π*-antibonding character for the central double bond and some delocalisation into the *p*-nitrophenyl groups. The presence of a surprisingly strong ethylenic π* character in the LUMO of TEE **6** has also been observed in the study of the electrochemical reduction behaviour.[15a] The HOMO of the D–A substituted (*E*)-**7** clearly exhibits π-bonding character that is delocalised over the TEE core and the donor substituent [Fig. 1(*c*)]. In the LUMO of (*E*)-**7**, delocalisation over the TEE core into the acceptor moiety is observed. Both frontier orbitals are concentrated about the central olefinic bond. In all three cases, the promotion of an electron from the HOMO to the LUMO therefore results in the elongation of this particular bond. Thus, the barrier to rotation is strongly reduced, enabling facile isomerisation.

Solvent dependence

The *trans–cis* isomerisation for D–A substituted TEE **7** was examined by irradiation of either the *cis*- or the *trans*-isomer at 451 nm in solvents of different polarity at 27 °C (Table 2). With the exception of $CHCl_3$, in which isomerisation rates were lower than expected, the photoequilibrium constant K^{eq}_{photo} steadily decreased with solvent polarity, and the photostationary state shifted increasingly towards the *trans*-isomer.

The partial quantum yields for **7** steadily diminished with increasing solvent polarity, and the total quantum yields became quite small (Table 2). The ratio $\Phi_{t\rightarrow c}/\Phi_{c\rightarrow t}$ also

decreased significantly with solvent polarity and correlated well with the dipole moments of the solvents. In the most polar solvents CH_3CN and DMF, $\Phi_{t\rightarrow c}$ was reduced to zero and (*E*)-**7** remained isomerically pure after irradiation for 115 min. The absence of isomerisation of (*E*)-**7** in CH_3CN and DMF precluded determination of $\Phi_{c\rightarrow t}$ from these reactions. Thus, independent measurements of $\Phi_{c\rightarrow t}$ starting from pure (*Z*)-**7** were conducted in these solvents. Irradiation of (*Z*)-**7** in CH_3CN at λ_{max} (473 nm) resulted in no isomerisation after 20 min. At slightly higher energy (451 nm), $\Phi_{c\rightarrow t}$ remained negligible after irradiation at maximum light intensity[18] for more than 1 h, with insufficient conversion to (*E*)-**7** for calculation of $\Phi_{c\rightarrow t}$ outside experimental error. Irradiation of (*E*)-**7** at a significantly shorter wavelength (291 nm) did induce isomerisation and afforded $\Phi_{t\rightarrow c} = 0.022$ and $\Phi_{c\rightarrow t} = 0.019$. At this higher energy, however, decomposition was eventually observed following continued irradiation at the photostationary state. Negligible isomerisation of (*Z*)-**7** was also seen in DMF ($\lambda_{exc} = 451$ nm).

The total quantum yield Φ_{total} showed a substantial decrease as a function of solvent polarity. This can be explained by the significantly higher dipole moments of (*Z*)- and (*E*)-**7** in the excited state as compared to the ground state, resulting from intramolecular D–A charge transfer. These highly polar states are strongly solvated by polar solvent molecules; hence, the tendency towards geometric isomerisation, which requires complete reorganisation of the solvent structure (and thus is dependant on the solvent relaxation time), is low.

The ratio of the partial quantum yields $\Phi_{t\rightarrow c}/\Phi_{c\rightarrow t}$ also decreases with increasing solvent polarity. The resulting formation of more *trans*-isomer can be explained again by solvent stabilisation. In non-polar solvents, the photostationary equilibrium favours formation of the *cis*-isomer due to more favourable dipolar interactions. In the more polar solvents, the *trans*-isomer also encounters substantial stabilisation through solvation, which reduces its propensity to isomerise into the *cis*-form.

Anomalous behaviour was observed in $CHCl_3$. The quantum yields for *trans–cis* isomerisation in this solvent of reduced polarity were similar to those measured in EtOH and not, as expected, to those in CCl_4 and THF. The *trans–cis* isomerisation showed clean isosbestic points, and no degradation products were observed in the HPLC analysis of the equilibrium mixture of **7** in this solvent. The possibility that this deviation arises from the presence of EtOH, used as a stabiliser in commercial $CHCl_3$, was discounted; a control isomerisation experiment using CCl_4 containing *ca.* 1% added EtOH ultimately revealed no rate retardation as compared to pure CCl_4.

The solvent dependence of the *trans–cis* isomerisation of D–A substituted TEE **7** sharply contrasts with the behaviour of DANS (**9**) which already shows $\Phi_{t\rightarrow c} = 0$ in EtOH.[22] Furthermore, the partial quantum yields $\Phi_{c\rightarrow t}$ in the case of DANS and stilbene are essentially solvent independent.[22] This has often been interpreted as an indication that long-lived intermediates, with concomitant solvent rearrangement, are not involved in the major *cis*→*trans* reaction pathway.[8a] The different behaviour of **9** as compared to **7** could result from the steric interactions between the two phenyl rings in non-planar (*Z*)-DANS. These interactions ultimately favour formation of the *trans*–isomer in a polar stabilising medium, and *cis*→*trans* isomerisation of DANS occurs even in highly polar solvents such as DMF ($\Phi_{c\rightarrow t} = 0.15$).[22] Similar steric constraints do not exist in the bis-arylated tetraethynylethene **7**; in the absence of strain release as driving force, *cis*→*trans* isomerisation is no longer observed in polar solvents such as DMF or CH_3CN (Table 2) which stabilise both isomeric forms. This analysis demonstrates well that solvent effects in TEEs can be studied separately from steric influences, which is not the case for stilbenes.

Table 3 Temperature dependence of the photochemical *trans–cis* isomerisation of A–A substituted DEE **3**[a]

T/°C	% *trans*[b]	% *cis*[b]	K_{photo}^{eq}[c]	$\Phi_{t\rightarrow c}$	$\Phi_{c\rightarrow t}$	Φ_{total}	$\Phi_{t\rightarrow c}/\Phi_{c\rightarrow t}$
6.5	55.1	44.9	0.81	0.11	0.31	0.42	0.35
14.0	54.7	45.3	0.83	0.12	0.35	0.47	0.34
21.0	53.9	46.1	0.86	0.11	0.33	0.44	0.33
32.5	51.8	48.2	0.93	0.13	0.33	0.46	0.39
47.5	48.6	51.4	1.06	0.14	0.29	0.43	0.48
65.0	49.0	51.0	1.04	0.14	0.31	0.45	0.45

[a] $\lambda_{exc} = 372$ nm in 1,4-dichlorobutane. [b] At photostationary state. [c] Photoequilibrium constant.[19]

The dependence of $\Phi_{t\rightarrow c}$ and $\Phi_{c\rightarrow t}$ on the excitation wavelength for D–A substituted TEE **7** also significantly distinguishes this molecule from DANS. Studies of DANS at different irradiation wavelengths revealed that $\Phi_{t\rightarrow c}$ and $\Phi_{c\rightarrow t}$ are both independent of λ_{exc}, even if the irradiation involved different absorption bands.[22] In contrast, the partial quantum yields of **7** (Table 2) and tetrakis-arylated TEE **8** displayed a strong dependence on the irradiation wavelength. For instance, irradiating molecule (*E*)-**8** at 528 nm for 18 min caused negligible isomerisation,[18] whereas irradiation at higher energy ($\lambda_{exc} = 390$ nm) gave $\Phi_{total} = 0.015$ (Table 1).

The contrasting results in the photoisomerisation of D–A substituted TEEs and DANS are somewhat surprising considering that the lowest energy excited states of both molecules should be dominated by an intramolecular D–A charge transfer. For DANS, the independence of the excitation wavelength from the isomerisation quantum yields has often been advanced as evidence against an isomerisation from the lowest singlet excited state.[8a] The strong dependence on excitation wavelength now suggests that *trans–cis* isomerisation of D/A functionalised DEEs and TEEs follows a different mechanism than postulated for D/A-substituted stilbenes such as DANS.

Temperature dependence

The temperature dependence of the photoinduced *trans–cis* isomerisation was studied for the A–A substituted DEE **3**, which previously had been shown to undergo *cis*→*trans* interconversion upon electrochemical reduction.[15a] Under photochemical isomerisation conditions, *trans–cis* product distributions and thus the magnitudes of $\Phi_{t\rightarrow c}$ and $\Phi_{c\rightarrow t}$ can be influenced by a thermodynamic rotational barrier in the excited state.[8b,22] To investigate the magnitude of such a barrier to rotation, the photochemical *trans–cis* isomerisation of **3** was measured in 1,4-dichlorobutane at temperatures from 6.5 to 65 °C (Table 3). Examination of the *trans–cis* ratio over this temperature range showed only slight changes in the isomeric distribution, as the amount of (*E*)-**3** present at the photostationary state decreases from 55 to 49%. Correspondingly, the photoequilibrium constant K_{photo}^{eq} for the isomerisation process increases only slightly from 0.81 to 1.04. Due to the uncertainties in the determination of $\Phi_{t\rightarrow c}$ and $\Phi_{c\rightarrow t}$, the partial quantum yields for **3** can be considered independent of temperature over the range investigated. Therefore, a significant thermal activation barrier is not involved in the photochemical isomerisation process.

Control experiments within the same temperature range revealed that there is no competing thermal *trans–cis* isomerisation involved. Thus, the results for A–A substituted **3** mirror the behaviour of 4-nitrostilbene which showed no change in $\Phi_{t\rightarrow c}$ and $\Phi_{c\rightarrow t}$ over a temperature range of 25 to −150 °C in the non-viscous solvent mixture of methylcyclohexane–isohexane (2 : 1 v/v).[21] The temperature independence of the partial quantum yields is of interest for device construction, where a stable optical behaviour within the temperature range of operation is desirable.

Conclusions

The photochemical *trans–cis* isomerisation of donor/acceptor substituted DEEs and TEEs showed a strong dependence on the pattern and degree of functionalisation, solvent polarity and excitation wavelength. The total quantum yield for photoisomerisation decreased in the series from A–A, to D–D and to D–A substituted derivatives. Photochemical *trans–cis* interconversion was significantly suppressed in a more highly functionalised bis-donor, bis-acceptor substituted TEE. Computational studies displayed strong π*-antibonding character for the central double bond in D–D, A–A and D–A substituted TEEs, which explains the facile photoisomerisation. A significant thermal activation barrier to photoisomerisation was not observed experimentally. D–A substituted arylated DEEs and TEEs, similar to DANS, prefer the *cis*-configuration upon irradiation in apolar solvents at room temperature, whereas for the symmetrically substituted DEEs and TEEs no preference for either isomer was found. However, important differences were also revealed between the two classes of chromophores. The photoisomerisation of the expanded chromophores is wavelength dependent which is not the case for stilbenes. Furthermore, the partial quantum yield $\Phi_{c\rightarrow t}$ for isomerisation of arylated DEEs and TEEs is strongly dependent on solvent polarity, whereas the corresponding isomerisation of stilbenes is unaffected by solvent. The results obtained in the photoisomerisation of stilbenes are strongly affected by the steric interactions in the non-planar *cis*-isomers. In contrast, as a result of their expanded conjugated carbon frames, arylated DEEs and TEEs are planar in both isomeric forms and isomerisation quantum yields depend exclusively on electronic and solvent effects. Thus, the DEE and TEE derivatives allow investigation and quantification of the latter effects separated from steric influences. None of the investigated compounds showed a tendency to undergo thermally induced isomerisation. This sets them further apart from functionalised (*Z*)-stilbene derivatives which can easily undergo a thermal reaction to the *trans*-form. The strong dependence of the isomerisation process on solvent polarity and excitation wavelength allows versatile manipulation and fine-tuning of the interconversion around the olefinic bond in DEEs and TEEs. These characteristics should make them very suitable for the construction of photochemically driven switches and hinges.

Experimental

General

Solvents were HPLC or spectroscopic grade (Aldrich or Fluka) and were used as received except for 1,4-dichlorobutane (Sigma) which was distilled prior to use. When appropriate, solvents were degassed by a minimum of three freeze–pump–thaw cycles and the solutions transferred to sealed cuvettes under argon. Compounds (*E*)-**2**, (*E*)-**4**–(*E*)-**8** and (*Z*)-**7** were prepared as previously described.[14a] HPLC separations were performed on a Hewlett Packard HP 1090 liquid chromatograph equipped with a diode array detector (DAD). Monochromatic sample irradiation in a 1 × 1 × 3 cm quartz cell from Hellma was carried out using a SPEX-1680 Fluorolog 0.22 m double spectrometer equipped with an Osram XBO 450 W Xenon lamp (ozone free) and a stabilised power supply. To ensure homogeneity of the solution throughout the irradiation process, a small magnetic stirrer plate was placed below the thermostatted cell holder. Melting points (uncorrected): Büchi SMP-20 melting point apparatus. UV–VIS spectra: Varian Cary 5 spectrophotometer equipped with a thermostatted sample holder. IR spectra: Perkin-Elmer 1600 FTIR spectrometer. ^{1}H and ^{13}C NMR spectra: Bruker AMX 500 instrument at room temperature, using residual $CHCl_3$ in the solvent $CDCl_3$ as lock and internal reference (7.24 ppm for ^{1}H and 77.0 ppm for ^{13}C NMR, respectively), *J* values are given in Hz. MS spectra: VG-Tribrid spectrometer. Elemental analyses: Mikrolabor in the Laboratorium für Organische Chemie at ETH Zürich.

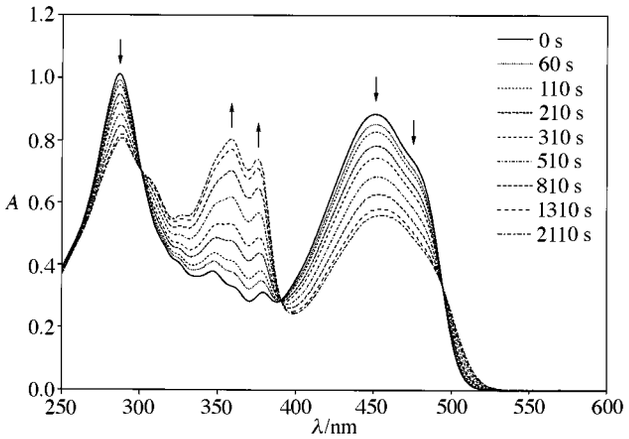

Fig. 2 Electronic absorption spectrum recorded during the photoisomerisation of (*E*)-**7** as a function of irritation time

Photoisomerisation procedures

General. All samples were irradiated at 27 °C with the exception of (*E*)-**3** in the variable temperature studies, where samples were thermostatted at the appropriate temperature throughout the entire experiment. All measurements were performed in non-degassed solvents. Control experiments using non-degassed solvents showed that irradiation at the longest wavelength maximum (λ_{max}) caused no detectable decomposition before reaching the photostationary states. For (*E*)-**2**, however, decomposition was always observed following irradiation, despite the use of degassed *n*-hexane. All experiments with compounds showing rapid isomerisation [(*E*)-**3** and (*E*)-**6**] were carried out using only red light for illumination, whereas all other derivatives tolerated incandescent light of low intensity without observable changes in their UV–VIS spectra. Data for all isomerisation experiments and an outline of the mathematical methods employed for data evaluation can be found in the Supplementary Material.‡

Typical procedure. A solution (*ca.* 2–4 × 10^{-5} M) of an isomerically pure compound was placed into a quartz cuvette equipped with a magnetic stirring bar. Preliminary irradiation and analysis were used to adjust the monochromatic light intensity for each molecule in order to afford isomerisation to the photostationary state (PS) within a reasonable time period (usually not more than 2 h). A series of UV–VIS spectra were then taken over a full range (250–600 nm) as a function of irradiation time until the PS was reached (Fig. 2). Plots of absorbance $A_{\lambda_{obs}}$ *vs.* time *t* at different analysis wavelengths λ_{obs} (typically four, *vide infra*) were examined to confirm achievement of the PS (Fig. 3). Following attainment of the PS and measurement of the final absorption spectrum, the irradiated solution was kept in the dark for at least 12 h and the absorptions at different λ_{obs} were remeasured. For all six compounds (*E*)-**3**–(*E*)-**8** investigated in this study, there were no observed changes from the PS absorption values, thus precluding participation of a competitive, thermal *trans–cis* isomerisation during the investigation.

After every isomerisation reaction, extinction diagrams[26] were constructed by plotting absorbance at one of the analysis

‡ A derivation of the mathematical relations used and experimental conditions for the *trans–cis* photoisomerisations and the solvent and temperature dependence studies of individual chromophores are available as supplementary material (SUPPL. No. 57332, 22 pp.). For details of the Supplementary Publications Scheme see 'Instructions for Authors', *J. Chem. Soc.*, *Perkin Trans. 2*, available *via* the RSC Web page (http://chemistry/rsc.org/authors).

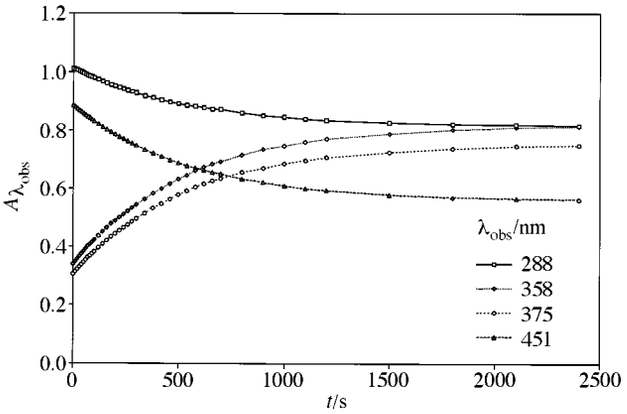

Fig. 3 Plot of absorption *vs.* irradiation time for (*E*)-**7** at four observation wavelengths (λ_{obs}) confirming attainment of the photostationary state

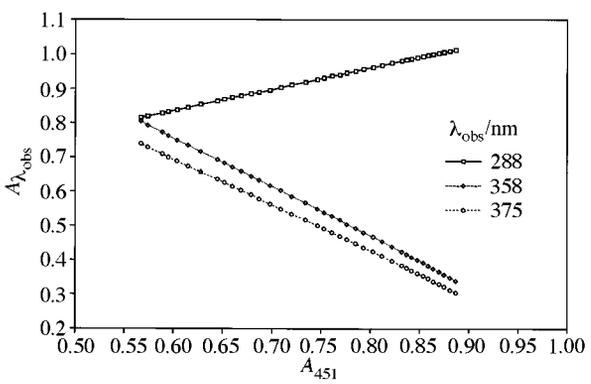

Fig. 4 Extinction diagram of (*E*)-**7** showing linear dependence of the different λ_{obs} values

wavelengths (*e.g.* $\lambda_{obs} = 451$ nm, Fig. 4) as a function of the other analysis wavelengths to prove uniformity of the *trans–cis* isomerisation. Experiments were discarded if clear isosbestic points were not obtained [*e.g.* in experiments with photodecomposing (*E*)-**2**], or if the extinction diagrams produced non-linear relationships.

The photoisomerisation kinetics were determined as follows: a stirred solution of (*E*)-**3**–(*E*)-**8** (3 cm^3) was irradiated at λ_{exc} for the appropriate time. The irradiated solution was then removed from the irradiation chamber in the dark (red light), and the absorptions at different wavelengths (λ_{obs}) were measured immediately. The observation wavelengths λ_{obs} for each molecule were chosen at points in the respective UV–VIS spectrum where absorbances of *trans*- and *cis*-isomers displayed the greatest disparity. The irradiation/absorbance measurement process was then continued until the photostationary state was reached, albeit more frequently during initial stages of the isomerisation when greater changes were observed. After reaching the PS, a small sample of the solution was removed and stored in the dark (−20 °C) for subsequent HPLC analysis of the equilibrium *trans–cis* isomeric concentrations. The irradiation/absorbance measurements were conducted twice for (*E*)-**3**, (*E*)-**4**, (*E*)-**6**–(*E*)-**8** and once for (*E*)-**5** in the structure–function studies with *n*-hexane as solvent (affording *ca.* 40 data points per λ_{obs}). The solvent and temperature dependence studies were performed once for each compound (affording *ca.* 20 data points per λ_{obs}).

Calculation of first-order rate constants. The determination of first-order reaction constants $k_{t\rightarrow c}$ and $k_{c\rightarrow t}$ required accurate knowledge of the photoequilibrium concentrations of each isomer in the reaction mixture. These were obtained by HPLC analysis of the irradiated solution using a SiO_2 stationary phase (Nucleosil-100, Knauer) and *n*-hexane–ethyl acetate mixtures (*ca.* 95:5) as the mobile phase. In each case, λ_{max} of the *trans*-isomer served as the detection wavelength of the DAD. In order to obtain a calibration curve concentration *vs. trans*-peak area for each compound, a dilution-row (1:0, 4:1, 3:2, 1:1) of four different concentrations of pure *trans*-compound was prepared, and each solution was measured five times. A straight calibration line was then fitted to obtain the relationship between concentration and *trans*-peak area. Each sample was measured five times, and the equilibrium concentration of the *trans*-compound C_t^{eq} was obtained from the resulting *trans*-peak areas using the calibration curve. The concentration of the photoequilibrium *cis*-isomer C_c^{eq} could then be calculated from the difference between the initial concentration of the *trans*-isomer C_t^0 and C_t^{eq}. The relative precision claimed for the evaluation of the equilibrium concentrations was better than 2% in all cases. To assure accuracy in the determination of concentrations, the calibration curve for the DAD was repeated as above for each different solvent utilised in the isomerisation reaction.

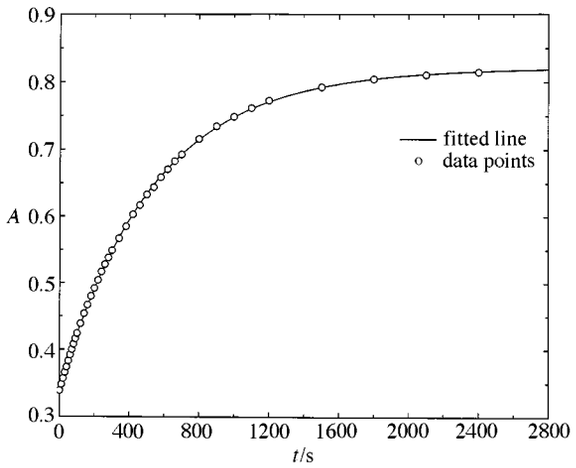

Fig. 5 Absorption *vs.* time diagram for (*E*)-**7** and the non-linear fit to eqn. (1) affording the overall rate constant k

Assuming a first-order rate law, the time dependent UV–VIS data at the four λ_{obs} (*vide supra*) are related to the overall rate constant k by eqn. (1), where $A_{\lambda_{obs}}(t)$ is the time-dependent

$$A_{\lambda_{obs}}(t) = \varepsilon_t C_t^{eq} + \varepsilon_c C_c^{eq} + (\varepsilon_c - \varepsilon_c) C_c^{eq} e^{-kt} \qquad (1)$$

absorbance of the reaction mixture at λ_{obs}, and ε_t and ε_c are the molar extinction coefficients of the pure *trans*- and *cis*-isomers at the wavelength of observation, respectively. The overall rate constants k were then obtained by applying an exponential fit to eqn. (1) (Fig. 5).[27]

The well-known linearisation methods for the calculation of k introduced by Guggenheim[26a,b,28] and Swinbourne,[26a,b,29] as well as the formal integration method[26a,b,30] of Mauser all provided results comparable to those of the non-linear method above.

Light intensity. The intensity of the monochromatic light was determined by the ferrioxalate actinometric method of Hatchard and Parker.[31] The $K_3Fe(C_2O_4)_3$ concentration of the standard solution was 0.006 M for λ_{exc} = 360, 390, 405, 416 nm and 0.15 M in the case of λ_{exc} = 450 and 451 nm. A two-point calibration was carried out, doubling the irradiation time in the second run. Thus, 3 cm^3 of the actinometric solution were put into a spectrophotometer cell identical to that of the photoisomerisation reaction and irradiated under exactly the same conditions as subsequent measurements. Of each irradiated solution, a 1 cm^3 sample was diluted with an aq. phenanthroline solution (0.2 M, 2 cm^3), acetate buffer (0.5 cm^3) and water to 10 cm^3 in a volumetric flask. Both solutions were stored in the dark (red light) for 30 min, and the absorption at 510 nm was then measured. The time of irradiation was adjusted to give a final background corrected absorption of the two irradiated solutions in the range 0.2–1.0. From these two independent absorption

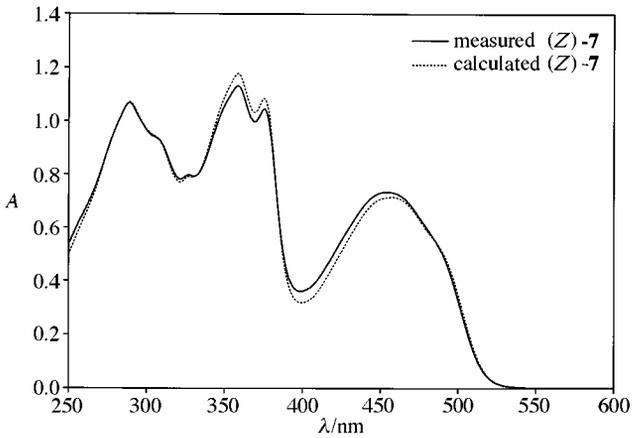

Fig. 6 UV–VIS spectrum for (*Z*)-**7** calculated from eqn. (4) and compared to the experimentally measured spectrum

values, the light intensity I_0 in E s^{-1} cm^{-2} was calculated for each λ_{exc}.

Calculation of quantum yields. The calculation of partial quantum yields was carried out as described in the literature.[26] Using the known quantities C_t^{eq} and C_c^{eq} and the overall rate constant k [eqn. (1)], the partial rate constants for the forward $k_{t\rightarrow c}$ and the backward reaction $k_{c\rightarrow t}$ could be determined from eqns. (2) and (3). In cases where the UV–VIS spectrum

$$k = k_{t\rightarrow c} + k_{c\rightarrow t} \quad (2)$$

$$K_{photo}^{eq} = \frac{C_c^{eq}}{C_t^{eq}} = \frac{k_{t\rightarrow c}}{k_{c\rightarrow t}} \quad (3)$$

of the pure *cis*-isomer was not available, the molar decadic extinction coefficient for the *cis*-isomer ε_c, required for the calculation of $\Phi_{c\rightarrow t}$, was calculated from eqn. (4), where $A_{\lambda_{exc}}^{eq}$ is

$$\varepsilon_c = \frac{A_{\lambda_{exc}}^{eq} - \varepsilon_t C_t^{eq}}{C_c^{eq}} \quad (4)$$

the absorbance at λ_{exc} at the photostationary state. Eqn. (4) could also be used to generate the entire spectrum of the *cis*-isomer of **7** as shown in Fig. 6. This method is particularly beneficial in cases where the *cis*-isomer is not easily accessible, such as (*Z*)-**6**, which is hardly separable from (*E*)-**6** on a preparative scale. A comparison between the calculated and experimental UV–VIS spectra for (*Z*)-**7** is also given in Fig. 6.

The partial quantum yields $\Phi_{t\rightarrow c}$ and $\Phi_{c\rightarrow t}$ are then given by eqns. (5) and (6), where I_0 is the intensity of the irradiation light

$$\Phi_{t\rightarrow c} = \frac{k_{t\rightarrow c}}{1000 I_0[(1 - 10^{-A_{\lambda_{exc}}^{eq}})/A_{\lambda_{exc}}^{eq}]\varepsilon_t} \quad (5)$$

$$\Phi_{c\rightarrow t} = \frac{k_{c\rightarrow t}}{1000 I_0[(1 - 10^{-A_{\lambda_{exc}}^{eq}})/A_{\lambda_{exc}}^{eq}]\varepsilon_c} \quad (6)$$

in E s^{-1} cm^{-2}. A complete description of the dynamics for a homogeneous stirred solution in a cuvette with parallel windows at constant monochromatic irradiation without scattering and reflection at the exit window is detailed in the literature.[32,33] For the quantum yields of isomerisation $\Phi_{t\rightarrow c}$ and $\Phi_{c\rightarrow t}$, a relative error (precision) of less than 3% is claimed, whereas the absolute error (accuracy) is *ca.* 10%. In cases where the isomerisation quantum yields are below 0.1, however, $\Phi_{t\rightarrow c}$ and $\Phi_{c\rightarrow t}$ are considered to be much less accurate.

(*E*)-1,6-Bis(4-nitrophenyl)-3,4-bis[(*tert*-butyldimethylsilyloxy)-methyl]hex-3-ene-1,5-diyne [(*E*)-3]

p-Iodonitrobenzene (0.17 g, 0.69 mmol), $[PdCl_2(PPh_3)_2]$ (0.010 g, 0.014 mmol), and CuI (0.003 g, 0.017 mmol) were added to a thoroughly degassed solution of (*E*)-3,4-bis[(*tert*-butyldimethylsilyloxy)methyl]hex-3-ene-1,5-diyne[14] (0.10 g, 0.28 mmol) in triethylamine (20 cm^3), and the solution was stirred for 18 h at room temp. The triethylamine was then removed *in vacuo*, sat. aq. NaCl solution was added (100 cm^3), and the mixture was extracted with CH_2Cl_2 (3 × 100 cm^3). The combined organic phases were dried over anhydrous $MgSO_4$ and concentrated *in vacuo.* Flash chromatography (SiO_2-H, *n*-hexane–ethyl acetate 5:1) and precipitation *via* addition of MeOH to a saturated CH_2Cl_2 solution gave (*E*)-**3** (0.11 g, 69%) as a yellow solid with mp 158–169 °C (Found: C, 63.42; H, 7.08; N, 4.51. $C_{32}H_{42}N_2O_6Si_2$ requires C, 63.33; H, 6.98; N, 4.62%); ν_{max}-$(CHCl_3)/cm^{-1}$ 2969m, 2933m, 2856m, 2359w, 2340w, 2207w, 1594s, 1522s, 1344s, 1256m, 1106m; $\lambda_{max}(CHCl_3)$/nm 372 (45 300); δ_H(500 MHz, $CDCl_3$) 0.13 (12 H, s), 0.92 (18 H, s), 4.61 (4 H, s), 7.58 (4 H, d, *J* 9.0), 8.21 (4 H, d, *J* 9.0); δ_C(125 MHz, $CDCl_3$) −5.08, 18.38, 25.84, 63.95, 91.45, 99.50, 123.76, 129.63, 130.59, 132.10, 147.28; *m*/*z* (EI, 70 eV) 607 (1, $[MH]^+$), 549 (100, $[M - Bu^t]^+$).

(*Z*)-1,6-Bis(4-nitrophenyl)-3,4-bis[(*tert*-butyldimethylsilyloxy)methyl]hex-3-ene-1,5-diyne [(*Z*)-3]

A solution of (*E*)-**3** (0.035 g, 0.058 mmol) in CH_2Cl_2 (100 cm^3) was irradiated in a quartz cell with monochromatic light (366 nm) for 2 h at room temp. Removal of the solvent *in vacuo* and flash chromatography (SiO_2-H, *n*-hexane–CH_2Cl_2 1:2) gave (*Z*)-**3** (0.013 g, 37%) in greater than 95% stereoisomeric purity as a yellow solid with mp 132–133 °C (Found: C, 63.42; H, 7.00; N, 4.53. $C_{32}H_{42}N_2O_6Si_2$ requires C, 63.33; H, 6.98; N, 4.62%). $\nu_{max}(CHCl_3)/cm^{-1}$ 2952m, 2930m, 2854m, 2253w, 2195w, 1595s, 1515s, 1346s, 1260m, 1108m; $\lambda_{max}(CHCl_3)$/nm 298 (20 700, sh), 314 (23 100), 368 (23 700); δ_H(500 MHz, $CDCl_3$) 0.13 (12 H, s), 0.92 (18 H, s), 4.45 (4 H, s), 7.57 (4 H, d, *J* 8.8), 8.19 (4 H, d, *J* 8.8); δ_C(125 MHz, $CDCl_3$) −5.20, 18.34, 25.82, 61.51, 94.33, 94.78, 123.78, 130.01, 131.44, 132.10, 147.24; *m*/*z* (EI, 70 eV) 607 (0.4, $[MH]^+$), 549 (66, $[M - Bu^t]^+$), 73 (100, $[SiMe_3]^+$).

Acknowledgements

We thank Dr S. Canonica for helpful discussions, the Rosenkranz Family Foundation for a research fellowship (to R. R. T.), and the Österreichischen Akademischen Austauschdienst and the ETH Zürich for an ERASMUS exchange grant (to J. B.). We acknowledge the generous allocations of computer resources by the ETH Zürich computer facilities.

References

1 (*a*) B. L. Feringa, W. F. Jager and B. de Lange, *J. Am. Chem. Soc.*, 1991, **113**, 5468; (*b*) B. L. Feringa, N. P. M. Huck and H. A. van Doren, *J. Am. Chem. Soc.*, 1995, **117**, 9929.
2 B. König, E. Schofield, P. Bubenitschek and P. G. Jones, *J. Org. Chem.*, 1994, **59**, 7142.
3 R. R. Naujok, H. J. Paul and R. M. Corn, *J. Phys. Chem.*, 1996, **100**, 10 497.
4 Z. Sekkat and M. Dumont, *Appl. Phys. B*, 1992, **54**, 486.
5 P. A. Jacobi, S. C. Buddhu, D. Fry and S. Rajeswari, *J. Org. Chem.*, 1997, **62**, 2894.
6 B. L. Feringa, N. P. M. Huck and A. M. Schoevaars, *Adv. Mater.*, 1996, **8**, 681.
7 H. Meier, *Angew. Chem.*, 1992, **104**, 1425; *Angew. Chem., Int. Ed. Engl.*, 1992, **31**, 1399.
8 (*a*) H. Görner and H. J. Kuhn in *Advances in Photochemistry*, ed. D. C. Neckers, D. H. Volman and G. von Bünau, Wiley-Interscience, New York, 1995, vol. 19, p. 1; (*b*) D. H. Waldeck, *Chem. Rev.*, 1991, **91**, 415; (*c*) D. Schulte-Frohlinde and H. Görner, *Pure Applied Chem.*, 1979, **51**, 279.
9 (*a*) S. Malkin and E. Fischer, *J. Phys. Chem.*, 1962, **66**, 2482; (*b*) A. M. Sanchez and R. H. de Rossi, *J. Org. Chem.*, 1996, **61**, 3446.
10 (*a*) W. Rettig, *Top. Curr. Chem.*, 1994, **169**, 253; (*b*) J.-F. Létard, R. Lapouyade and W. Rettig, *J. Am. Chem. Soc.*, 1993, **115**, 2441; (*c*) J. Saltiel, *J. Am. Chem. Soc.*, 1967, **89**, 1036.

11 *Inter alia*: (*a*) F. D. Lewis and J.-S. Yang, *J. Am. Chem. Soc.*, 1997, **119**, 3834; (*b*) J. E. Gano, P. A. Garry, P. Sekher, J. Schliesser and Y. W. Kim, *J. Am. Chem. Soc.*, 1997, **119**, 3826.
12 (*a*) L. Sun and H. Görner, *J. Phys. Chem.*, 1993, **97**, 11 186; (*b*) H. Gruen and H. Görner, *J. Phys. Chem.*, 1989, **93**, 7144; (*c*) H. Ephardt and P. Fromherz, *J. Phys. Chem.*, 1989, **93**, 7717.
13 (*a*) R. R. Tykwinski and F. Diederich, *Liebigs Ann./Recueil*, 1997, 649; (*b*) J. Anthony, A. M. Boldi, Y. Rubin, M. Hobi, V. Gramlich, C. B. Knobler, P. Seiler and F. Diederich, *Helv. Chim. Acta*, 1995, **78**, 13; (*c*) J. Anthony, C. B. Knobler and F. Diederich, *Angew. Chem.*, 1993, **105**, 437; *Angew. Chem., Int. Ed. Engl.*, 1993, **32**, 406; (*d*) F. Diederich and Y. Rubin, *Angew. Chem.*, 1992, **104**, 1123; *Angew. Chem., Int. Ed. Engl.*, 1992, **31**, 1101.
14 (*a*) R. R. Tykwinski, M. Schreiber, R. Pérez Carlón, F. Diederich and V. Gramlich, *Helv. Chim. Acta*, 1996, **79**, 2249; (*b*) R. R. Tykwinski, M. Schreiber, V. Gramlich, P. Seiler and F. Diederich, *Adv. Mater.*, 1996, **8**, 226; (*c*) J. Anthony, Ph.D. Thesis, University of California, Los Angeles, 1993.
15 (*a*) A. Hilger, J.-P. Gisselbrecht, R. R. Tykwinski, C. Boudon, M. Schreiber, R. E. Martin, H. P. Lüthi, M. Gross and F. Diederich, *J. Am. Chem. Soc.*, 1997, **119**, 2069; (*b*) C. Boudon, J. P. Gisselbrecht, M. Gross, J. Anthony, A. M. Boldi, R. Faust, T. Lange, D. Philp, J.-D. Van Loon and F. Diederich, *J. Electroanal. Chem.*, 1995, **394**, 187.
16 M. Schreiber, R. R. Tykwinski, F. Diederich, R. Spreiter, U. Gubler, Ch. Bosshard, I. Poberaj, P. Günter, C. Boudon, J.-P. Gisselbrecht, M. Gross, U. Jonas and H. Ringsdorf, *Adv. Mater.*, 1997, **9**, 339.
17 (*a*) Ch. Bosshard, R. Spreiter, P. Günter, R. R. Tykwinski, M. Schreiber and F. Diederich, *Adv. Mater.*, 1996, **8**, 231; (*b*) R. Spreiter, Ch. Bosshard, G. Knöpfle, P. Günter, R. R. Tykwinski, M. Schreiber and F. Diederich, *J. Phys. Chem.*, in the press.
18 The maximum light intensity was approximately 10^{-8} E s^{-1} cm^{-2}.
19 The concentrations of *trans*- and *cis*-isomers at the photostationary state are directly related to $\Phi_{t\rightarrow c}$ and $\Phi_{c\rightarrow t}$ and the molar absorption coefficients ε_t and ε_c at the wavelength of irradiation λ_{exc}.[7,8a] From this a photoequilibrium constant can be defined by eqn. (i).

$$K_{photo}^{eq} = \frac{C_c^{eq}}{C_t^{eq}} = \frac{\Phi_{t\rightarrow c}\varepsilon_t}{\Phi_{c\rightarrow t}\varepsilon_c} \quad \text{(i)}$$

20 J. Saltiel and J. L. Charlton, cis–trans *Isomerization of Olefins*, in *Rearrangements in Ground and Excited States*, ed. P. de Mayo, Academic Press, New York, 1980, p. 25.
21 D. Gegiou, K. A. Muszkat and E. Fischer, *J. Am. Chem. Soc.*, 1968, **90**, 3907.
22 D. Schulte-Frohlinde, H. Blume and H. Güsten, *J. Phys. Chem.*, 1962, **66**, 2486.
23 J. L. Brédas, *Science*, 1994, **263**, 487.
24 AMPAC 5.0, Semichem, 7128 Summit, Shawnee, KS 66216, 1994.
25 G. W. C. Kaye and T. H. Laby, *Tables of Physical and Chemical Constants and Some Mathematical Functions*, Longman, London, 1973, p. 191.
26 See the following monographs on UV–VIS spectroscopy: (*a*) H.-H. Perkampus, *UV–VIS-Spektroskopie und ihre Anwendungen*, ed. W. Fresenius, J. F. K. Huber, E. Pungor, G. A. Rechnitz, W. Simon, G. Tölg and Th. S. West, Springer, Berlin, 1986; (*b*) J. Polster, *Reaktionskinetische Auswertung spektroskopicher Messdaten*, Vieweg, Braunschweig, 1995; (*c*) G. Gauglitz, *Photophysical, Photochemical and Photokinetic Properties of Photochromic Systems* in *Photochromism—Molecules and Systems*, ed. H. Dürr and H. Bouas-Laurent, Elsevier, Amsterdam, 1990, p. 15.
27 Non-linear fits were calculated using the software *pro Fit*, Ver. 5.0.0 for Power Macintosh, Quantum Soft, Zürich, 1990–96.
28 E. A. Guggenheim, *Philos. Mag.*, 1926, **2**, 538.
29 E. S. Swinbourne, *J. Chem. Soc.*, 1960, **473**, 2371.
30 (*a*) H. Mauser, *Z. Naturforsch.*, *Teil A*, 1964, **19**, 767; (*b*) H. Mauser, *ibid.*, 1983, **38**, 359; (*c*) H. Mauser and U. Hezel, *Z. Naturforsch.*, *Teil. B*, 1971, **26**, 203.
31 (*a*) C. A. Parker, *Proc. R. Soc. London*, *A*, 1953, **220**, 104; (*b*) C. G. Hatchard and C. A. Parker, *Proc. R. Soc. London*, *A*, 1956, **235**, 518; (*c*) S. L. Murov, *Handbook of Photochemistry*, Marcel Dekker, New York, 1973, p. 119; (*d*) J. N. Demas, W. D. Bowman, E. F. Zalewski and R. A. Velapoldi, *J. Phys. Chem.*, 1981, **85**, 2766.
32 H. Mauser, *Formale Kinetik*, Bertelsmann, Düsseldorf, 1974.
33 G. Gauglitz, *J. Photochem.*, 1976, **5**, 41.

Paper 7/07679G
Received 24*th October* 1997
Accepted 13*th November* 1997